

**THE FRAGILITY OF HIGH- p_T HADRON SPECTRA
AS A HARD PROBE**K.J. Eskola^{a,b,1}, H. Honkanen^{a,b,2}, C.A. Salgado^{c,3} and U.A. Wiedemann^{c,4}^a*Department of Physics,
P.O.Box 35, FIN-40014 University of Jyväskylä, Finland*^b*Helsinki Institute of Physics,
P.O.Box 64, FIN-00014 University of Helsinki, Finland*^c*Department of Physics, CERN, Theory Division,
CH-1211 Geneva 23, Switzerland***Abstract**

We study the suppression of high- p_T hadron spectra in nuclear collisions, supplementing the perturbative QCD factorized formalism with radiative parton energy loss. We find that the nuclear modification factor $R_{AA}(p_T)$, which quantifies the degree of suppression, is almost p_T -independent both for RHIC (in agreement with data) and for the LHC. This is a consequence of the shape of the partonic p_T -spectrum in elementary collisions which implies that for the same value of R_{AA} at higher p_T , an increasingly smaller fraction of parton energy loss is needed. When the values of the time-averaged transport coefficient \hat{q} exceed $5 \text{ GeV}^2/\text{fm}$, $R_{AA}(p_T)$ gradually loses its sensitivity to the corresponding produced energy density. This is due to particle production in the outer corona of the medium, which remains almost unsuppressed even for extreme densities. Thus, even for the highest experimentally accessible transverse momentum at the LHC and in contrast to jets, the measurement of leading partons via leading hadrons is not a penetrating probe of the dense matter, but a rather fragile probe which fragments for the opacities reached below the skin of the medium. Relating the transport coefficient to the energy density produced in the collision region, we find and discuss a phenomenon reminiscent of the opacity problem of elliptic flow: namely, the interaction of the hard parent parton with the medium appears to be much stronger than that expected for perturbative interactions of the hard parton with an ideal quark gluon plasma.

¹kari.eskola@phys.jyu.fi²heli.honkanen@phys.jyu.fi³carlos.salgado@cern.ch⁴urs.wiedemann@cern.ch

1 Introduction

In Au+Au collisions at $\sqrt{s_{NN}} = 130$ and 200 GeV, experiments at the Relativistic Heavy Ion Collider, RHIC, observe a strong, a factor of 4-5, suppression of high- p_T leading hadron spectra [1, 2, 3, 4, 5, 6]. The centrality dependence of this effect, the corresponding suppression in leading back-to-back correlations [7], and the moderate enhancement and opposite centrality dependence observed in the same p_T -range in d +Au collisions [8, 9] are strong indications that the suppression is predominantly a final state effect in which the energy of high- p_T particles is degraded depending on the in-medium pathlength and the density of the produced medium. Formation time arguments [10] imply that for $p_T > 5 - 7$ GeV, this energy loss is of partonic origin while hadronization occurs *outside* the partonic medium. This is also supported by the disappearance of the particle species dependence of the suppression for $p_T > 5 - 7$ GeV. In this high- p_T regime, the suppression of hadrons is widely regarded as a “hard probe” for the characterization of the energy density of the medium produced in nucleus-nucleus collisions. Recent studies, based on medium-induced radiative parton energy loss [11, 12, 13, 14, 15, 16], quote time-dependent energy densities which at time $\tau_0 = 0.2$ fm/c after the collision lie a factor $\mathcal{O}(100)$ above the energy density of cold nuclear matter [17, 18].

In this paper, we calculate the nuclear modification factor for high- p_T hadronic spectra in nuclear collisions,

$$R_{AA}(p_T, y) = \frac{d^2 N^{AA}/dp_T dy}{\langle T_{AA} \rangle_c d^2 \sigma^{NN}/dp_T dy}. \quad (1)$$

Here, $\langle T_{AA} \rangle_c$ is the standard nuclear overlap function, calculated as the average in the measured centrality class. In the absence of nuclear or medium effects, $R_{AA} \equiv 1$. The starting point of our calculation is the collinearly factorized leading order (LO) perturbative QCD formalism which reproduces the shape of the hadronic high- p_T spectrum $d^2 \sigma^{NN}/dp_T dy$ in proton-proton collisions at RHIC energies [19]. Our discussion will be limited to $p_T \gtrsim 5$ GeV. In the calculation of the charged hadron spectrum $d^2 N^{AA}/dp_T dy$ in this range, we include both initial and final state effects. Nuclear modifications to parton distribution functions are taken from the EKS98 parametrization [20] and isospin effects are included as in [19]. As a medium effect, we consider partonic final state energy loss, which is introduced via the quenching weights $P_f(\Delta E, L, \hat{q})$ calculated in Ref. [21]. The quenching weights will be discussed in more detail in section 2.1. They denote the probability that a hard parton f radiates an additional medium-induced amount of energy ΔE if it propagates through a medium of length L . The quenching weight depends on the transport coefficient \hat{q} which is determined by the average transverse momentum squared transferred to the projectile parton per unit pathlength, $\hat{q} = \langle q_T^2 \rangle / \lambda$. It characterizes the energy density of the medium, $\hat{q} \propto \epsilon^{3/4}$ [22]. With this input, the hadron spectrum in nucleus-nucleus

collisions reads schematically

$$d\sigma_{(\text{med})}^{AA \rightarrow h+X} = \sum_f d\sigma_{(\text{vac})}^{AA \rightarrow f+X} \otimes P_f(\Delta E, L, \hat{q}) \otimes D_{f \rightarrow h}^{(\text{vac})}(z, \mu_F^2). \quad (2)$$

Here,

$$d\sigma_{(\text{vac})}^{AA \rightarrow f+X} = \sum_{ijk} f_{i/A}(x_1, Q^2) \otimes f_{j/A}(x_2, Q^2) \otimes \hat{\sigma}_{ij \rightarrow f+k} \quad (3)$$

and $f_{i/A}(x, Q^2)$ are the nuclear parton distribution functions and $\sigma_{ij \rightarrow f+k}$ the perturbatively calculable partonic cross sections.

The paper is organized as follows. In Section 2 we give details of the formalism used to compute hadron spectra with parton energy loss. Results for Au+Au collisions at $\sqrt{s_{\text{NN}}} = 200$ GeV are presented in Section 3 and predictions for the LHC are given in Section 4. In Section 5, we discuss the nuclear modification factor for Au+Au collisions at intermediate energy $\sqrt{s_{\text{NN}}} = 62.4$ GeV, where data are just being analyzed. In Section 6, we discuss in detail how the main model parameter of our analysis, the time-averaged transport coefficient \hat{q} , is related to the energy density produced in the medium. The main conclusions are summarized in Section 7. The results for RHIC and for the LHC are further explored in Appendix A.

2 Framework

2.1 Quenching weights

Under the assumption that multiple gluons are emitted independent of each other, the probability that a parton loses an amount ΔE of its energy by medium-induced gluon radiation is [23],

$$P(\Delta E) = \sum_{n=0}^{\infty} \frac{1}{n!} \left[\prod_{i=1}^n \int d\omega_i \frac{dI(\omega_i)}{d\omega} \right] \delta \left(\Delta E - \sum_{i=1}^n \omega_i \right) \exp \left[- \int d\omega \frac{dI}{d\omega} \right]. \quad (4)$$

This probability distribution has been calculated and tabulated [21] for the medium-induced gluon energy distribution $\omega \frac{dI}{d\omega}$ of a hard parton. [In the present study, we use a probability distribution calculated with $\alpha_S = 0.5$ instead of $\alpha_S = 1/3$. Since $\Delta E \propto \alpha_s \hat{q}$, the dependence on the value of the coupling constant can be largely absorbed in a rescaling of \hat{q} .] The calculation of Ref. [21] was done in two approximations which differ in viewing the medium as a source of many soft [12, 13, 14] or a few hard [14, 15] momentum transfers, respectively. For the purpose of the present study, the small numerical differences between both approximations are not important [21]. We use the soft multiple scattering approximation, where the quenching weights $P(\Delta E)$ depend on the parton species (light quark or gluon), the in-medium pathlength L and the

transport coefficient \hat{q} . For a static medium, \hat{q} does not show a time-dependence. Extension and density of the medium can be expressed in terms of the characteristic gluon frequency $\omega_c = \frac{1}{2}\hat{q}L^2$ and the dimensionless quantity $R = \omega_c L$.

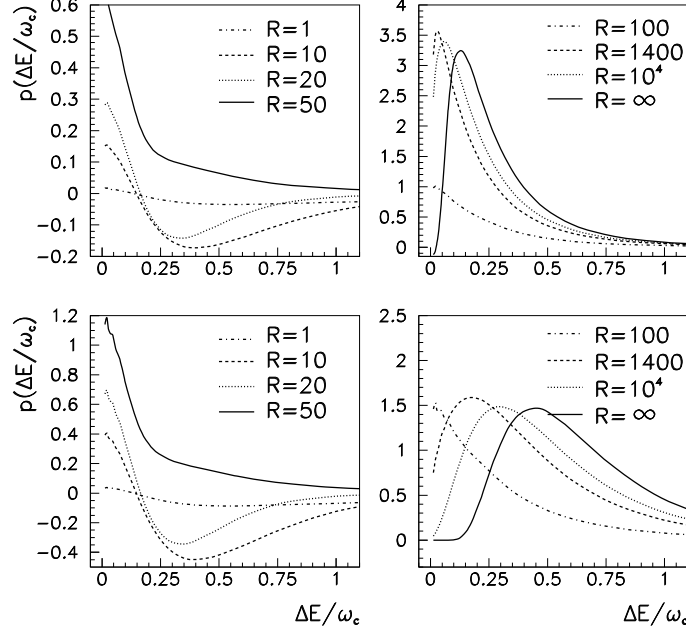


Figure 1: Continuous part of the quenching weights for light quarks (upper row) and gluons (lower row) computed in the multiple soft scattering approximation with $\alpha_S = 0.5$.

In general, the density of the medium decreases strongly in time due to longitudinal and transverse expansion. Hence, the transport coefficient should be time-dependent. However, the gluon energy distribution $\omega \frac{dI}{d\omega}$ for a time-dependent transport coefficient \hat{q}_τ agrees with the energy distribution obtained for an *equivalent static* linear line-averaged transport coefficient [24, 25]

$$\hat{q} = \frac{2}{L^2} \int_{\tau_0}^{\tau_0+L} \tau \hat{q}_\tau(\tau) d\tau. \quad (5)$$

Here, τ_0 is the time at which the parton is produced and for $\tau_0 \ll L$, the τ_0 -dependence of \hat{q} is numerically negligible. This allows us to base our analysis on an equivalent static scenario and to translate afterwards with Eq. (5) the values for the time-averaged \hat{q} into time-dependent transport coefficients.

The probability distribution $P(\Delta E/\omega_c, R)$ consists of a discrete and a continuous part (see Figs. 1 and 2)

$$P(\Delta E/\omega_c, R) = p_0(R)\delta(\Delta E/\omega_c) + p(\Delta E/\omega_c, R). \quad (6)$$

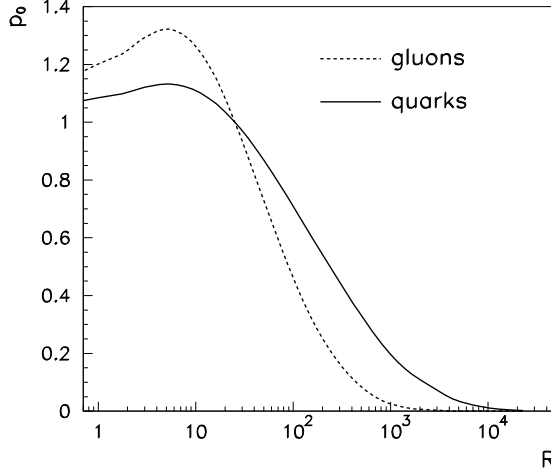


Figure 2: Discrete part of the quenching weights for light quarks and gluons computed in the multiple soft scattering approximation with $\alpha_S = 0.5$.

The continuous part denotes the probability to lose an additional energy ΔE due to medium induced gluon radiation. The discrete contribution p_0 is the finite probability for the projectile to escape the collision region of finite size and finite opacity without further interaction [24]. The quenching weight $P(\Delta E/\omega_c, R)$ is normalized to unity,

$$\int_0^\infty d(\Delta E/\omega_c) P(\Delta E/\omega_c, R) = p_0(R) + \int_0^\infty d(\Delta E/\omega_c) p(\Delta E/\omega_c, R) = 1. \quad (7)$$

$P(\Delta E/\omega_c, R)$ is a generalized probability. It can take negative values since it describes a medium-induced redistribution of gluon radiation which - compared to the gluon radiation in the vacuum - can be *reduced* in some range of phase space [26].

The quenching weights are computed in the eikonal limit of very large initial parton energy E_i . For the case of realistic initial parton energies, finite energy corrections have to be taken into account. In the absence of a formalism which includes them a priori, this is done by ensuring with kinematic cuts that the probability distribution $P(\Delta E/\omega_c, R)$ has weight only in the range $\Delta E < E_i$ [23, 27, 28, 29]. To illustrate the theoretical uncertainty associated with finite energy corrections, we shall compare results without such corrections to results obtained from the reweighted (‘rw’) probability [28]

$$P_{\text{rw}}(\Delta E/\omega_c, R) = \frac{P(\Delta E/\omega_c, R)}{\int_0^{E_i/\omega_c} d(\Delta E/\omega_c) P(\Delta E/\omega_c, R)} \Theta(1 - \Delta E/E_i). \quad (8)$$

We consider the non-reweighted result for the ratio R_{AA} as a lower limit.

Numerically, we have checked that the effect of reweighting (8) is comparable to the finite energy corrections in other approaches [27] where kinematic cuts are imposed on the level of the gluon energy distribution by multiplying with the vacuum splitting function.

2.2 Hadron spectra with parton energy loss

We first discuss the nuclear geometry entering the calculation of the nuclear modification factor (1). The centrality dependence is taken into account by defining an effective nucleus A_{eff} for which the number of participants in central $A_{\text{eff}} + A_{\text{eff}}$ collision equals $\langle N_{\text{part}}^{AA} \rangle_c$. Here, the number of participants is obtained from an optical Glauber analysis with realistic Wood-Saxon (WS) profile for the centrality class c [30]. As far as energy loss is concerned, the A_{eff} nucleus is assumed to be cylindrical and uniform, but we correct the final spectra for the difference between $T_{A_{\text{eff}} A_{\text{eff}}}^{\text{cyl}}(0)$ and $T_{A_{\text{eff}} A_{\text{eff}}}^{\text{WS}}(0)$.

The partons produced at midrapidity $y = 0$ propagate in the transverse plane. Consider a parton which is produced at a position $\vec{s} = (s, \phi_S)$ with respect to the transverse coordinates and which propagates in the transverse direction given by the angle ϕ_L . Its angle of propagation with respect to \vec{s} is $\phi_{LS} = \phi_L - \phi_S$. The geometrical transverse path length L_{geom} for this parton is

$$L_{\text{geom}}(s, \phi_{LS}) = -s \cos \phi_{LS} + \sqrt{s^2 \cos^2 \phi_{LS} + R_{A_{\text{eff}}}^2 - s^2}, \quad (9)$$

where $R_{A_{\text{eff}}}$ is the radius of A_{eff} . We assume that significant energy loss occurs only in the dense QGP-phase whose estimated lifetime τ_{QGP} may be shorter than L_{geom} . Therefore the in-medium path length which enters the quenching weight (5) is chosen to be $L = \min(L_{\text{geom}}, L_{\text{cut}} \sim \tau_{\text{QGP}})$. Varying L_{cut} will turn out to be a useful tool to establish to what extent particle emission is surface dominated.

We compute the inclusive production of charged particles at midrapidity in the framework of factorized leading-order partonic cross sections, using nuclear parton distributions, fragmentation functions and quenching weights but no intrinsic transverse momenta. As in [19] the renormalization and factorization scales are set to $\mu = Q = q_T$ and fragmentation scale to $\mu_F = p_T$, where q_T and p_T are the transverse momentum of the parton and hadron, respectively. We use CTEQ5 parton distributions [31] with nuclear effects for A_{eff} from EKS98 [20], and KKP fragmentation functions [32]. The $p + p$ reference spectra are obtained as in [19].

The inclusive cross section for the production of a parton of flavour f and an initial transverse momentum q_{T_i} and rapidity y_i is given e.g. in Eqs. (4) and (5) of [19]. When traversing a medium, the parton will lose a fraction ϵ of its initial energy E_i , but it will not change significantly the direction of its trajectory, $\phi_i \equiv \phi_{LS}$. Therefore,

we can write for the spectrum of the outgoing partons

$$\begin{aligned} \frac{dN^{AA \rightarrow f+X}}{d^2 s dq_{T_f} d\phi_f dy_f} &= [T_A(s)]^2 \int_0^1 d\epsilon P(\epsilon, L, \hat{q}) \int d^2 q_{T_i} dy_i \frac{d\sigma^{AA \rightarrow f+X}}{d^2 q_{T_i} dy_i} \\ &\quad \times \delta(y_f - y_i) \delta(\phi_f - \phi_i) \delta(q_{T_f} - (1 - \epsilon)q_{T_i}) \\ &\quad \times \Theta(0 \leq \phi_i \leq 2\pi) \\ &\quad \times \Theta\left(q_0 \leq q_{T_i} \leq \frac{\sqrt{s}}{2 \cosh y_i}\right) \Theta\left(|y_i| \leq \text{arcosh} \frac{\sqrt{s}}{2q_0}\right), \end{aligned} \quad (10)$$

where $T_A(s) = \frac{A}{(\pi R_A^2)} \Theta(R_A^2 - s^2)$, q_0 is the lower limit for the *initial* partonic transverse momentum and $P(\epsilon, L, \hat{q})$ is the quenching weight. In our notation $\Delta E = \epsilon E_i = \epsilon q_{T_i} \cosh y_i$, so

$$P(\epsilon, L, \hat{q}) = \frac{E_i}{\omega_c} P(\Delta E / \omega_c, R) \quad (11)$$

and

$$P_{\text{rw}}(\epsilon, L, \hat{q}) = \frac{\frac{E_i}{\omega_c} P(\Delta E / \omega_c, R)}{\int_0^{E_i/\omega_c} d(\Delta E / \omega_c) P(\Delta E / \omega_c, R)}. \quad (12)$$

From Eq. (10) we find that

$$\max(0, 1 - q_{T_f}/q_0) \leq \epsilon \leq 1 - \frac{2q_{T_f} \cosh y_f}{\sqrt{s}} \quad (13)$$

and

$$\begin{aligned} \frac{dN^{AA \rightarrow f+X}}{dq_{T_f}^2 dy_f} &= \int_0^{R_A} ds s \int_0^{2\pi} d\phi_f \int d\epsilon P(\epsilon, L, \hat{q}) [T_A(s)]^2 \frac{1}{(1 - \epsilon)^2} \frac{d\sigma^{AA \rightarrow f+X}}{dq_{T_i}^2 dy_i} \\ &\quad \times \Theta\left(0 \leq q_{T_f} \leq \frac{\sqrt{s}}{2 \cosh y_f}\right) \Theta\left(|y_f| \leq \text{arcosh} \frac{\sqrt{s}}{2q_0}\right), \end{aligned} \quad (14)$$

with $q_{T_i} = q_{T_f}/(1 - \epsilon)$ and $y_i = y_f$.

We define z as the fraction of the energy of the parent parton carried by the leading hadron, $z = E_h/E_f$. For a hadron with transverse momentum p_T we obtain [19]

$$\frac{dN^{AA \rightarrow h+X}}{dp_T^2 dy} = K(\sqrt{s}) \cdot J(m_T, y) \sum_f \int \frac{dz}{z^2} D_{f \rightarrow h}(z, \mu_F^2) \frac{dN^{AA \rightarrow f+X}}{dq_{T_f}^2 dy_f}, \quad (15)$$

where

$$q_{T_f} = \frac{p_T}{z} J(m_T, y), \quad y_f = \text{arsinh} \left(\frac{m_T}{p_T} \sinh y \right) \quad (16)$$

and

$$J(m_T, y) = \left(1 - \frac{m^2}{m_T^2 \cosh^2 y} \right)^{-1/2}. \quad (17)$$

The integration region for z is

$$\frac{2m_T}{\sqrt{s}} \cosh y \leq z \leq 1, \quad (18)$$

since we do not attempt to explore the region $p_T < q_0$. The cms-energy dependent K -factors applicable within our framework were determined in [19]. They are important for the overall normalization of the spectrum but they cancel in the nuclear modification factor R_{AA} discussed in the next sections.

Our formalism is equivalent to defining medium-modified fragmentation function [24, 27, 33]

$$D_{f \rightarrow h}^{(\text{med})}(z, \mu_F^2) = \int d\epsilon P(\epsilon) \frac{1}{(1-\epsilon)} D_{f \rightarrow h} \left(\frac{z}{1-\epsilon}, \mu_F^2 \right). \quad (19)$$

Neglecting the masses, Eq. (15) simplifies [23] for the case of small ΔE and $z = E_h/E_f \sim 1$ to

$$\frac{dN^{AA \rightarrow h+X}}{dp_T dy} \sim \int d(\Delta E) P(\Delta E) \frac{dN^{(\text{vac})}(p_T + \Delta E)}{dp_T dy}. \quad (20)$$

Here, $dN^{(\text{vac})}/dp_T dy$ is the spectrum of hadrons in the case of no medium (i.e. it coincides with the proton-proton spectrum in the absence of initial state effects as shadowing etc.). The suppression computed with (20) gives a rather good approximation to the one computed with the full formula (15).

3 Results for RHIC at $\sqrt{s_{NN}} = 200$ GeV

Based on the above formalism, we have studied the nuclear modification factor $R_{AA}(p_T)$ for charged hadrons, $h \equiv (h^+ + h^-)/2$ in Au+Au collisions at $\sqrt{s_{NN}} = 200$ GeV. We include charged pions, kaons and (anti)protons in the sum of charged particles. Our discussion is limited to the 0 – 5% most central collisions. This centrality class corresponds to the head-on collision of an effective nucleus of size $A_{\text{eff}} = 181$.

In Fig. 3, we compare data from RHIC with the nuclear modification factor calculated for different values of the transport coefficient \hat{q} . This figure is for a medium which exists for at most $\tau \sim L_{\text{cut}} = 5$ fm in the dense partonic phase. We find that even in the absence of final state parton energy loss, $\hat{q} = 0$, the nuclear modification factor shows a reduction from the baseline $R_{AA} \equiv 1$ for $p_T \gtrsim 13$ GeV. The reason is that in this p_T region, the incoming parton momentum fractions $x \simeq \frac{2p_T/\langle z \rangle}{\sqrt{s}}$ sampled by the hadronic spectrum lie in the so-called EMC region where nuclear parton distribution functions decrease faster than free proton parton distribution functions with increasing x [20]. This decrease of the incoming parton flux translates into a p_T -dependent decrease of the nuclear modification factor R_{AA} . As the density of the medium (or equivalently the

transport coefficient) is increased, the nuclear modification factor is reduced further. This is caused by parton energy loss in the final state. Interestingly, the resulting nuclear modification factor R_{AA} is almost p_T -independent and its dependence on \hat{q} becomes weaker as \hat{q} increases. We now discuss these two features in more detail:

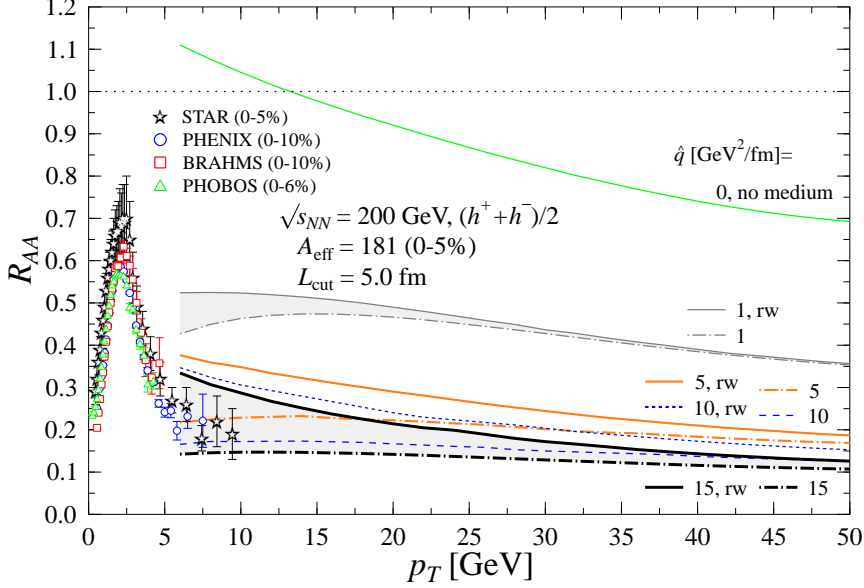


Figure 3: (Colour online) The nuclear modification factor R_{AA} for charged hadrons $h \equiv (h^+ + h^-)/2$ in the 0 – 5% most central Au+Au collisions at $\sqrt{s_{NN}} = 200$ GeV. Different lines are for a maximal lifetime of the medium $\tau \sim L_{\text{cut}} = 5$ fm and different values of the transport coefficient \hat{q} . The shaded region between the curves calculated with reweighted (solid curves) and non-reweighted (dotted-dashed curves) quenching weights is indicative of uncertainties related to finite energy corrections. For comparison, the most central R_{AA} data from the RHIC collaborations are shown (with statistical errors only): 0 – 5% STAR data for $|\eta| < 0.5$ [4], 0 – 10% PHENIX data for $|\eta| < 0.35$ [2], 0 – 10% BRAHMS data for $\eta = 0$ [6] and 0 – 6% PHOBOS data for $0.2 < \eta < 1.4$ [5].

To understand the approximate p_T -independence of R_{AA} , we study the sensitivity of R_{AA} to the p_T -dependent shape of the partonic cross section entering (2). (For qualitative results we assume $z \sim 1$, which is a fairly good approximation for quark dominated hadron production at RHIC in the large- p_T region of our interest.) We consider first a partonic cross section which has a powerlaw tail $d\sigma/dp_T \sim 1/p_T^n$, n constant. If n is sufficiently large, then the medium-modified spectrum can be obtained by shifting the vacuum spectrum by $S(p_T) \sim \sqrt{p_T/n}$ [23], and one finds $R_{AA}(p_T) \sim (1 + c/\sqrt{np_T})^{-n}$ where $c = \sqrt{2\pi\alpha_s^2\omega_c}$. In this case, R_{AA} approaches unity in the limit

of large p_T , except for possible modifications in the incoming parton distributions. In contrast, if the partonic spectrum is exponential, one finds a p_T -independent nuclear modification factor

$$R_{AA}(p_T) \sim \int d(\Delta E) P(\Delta E) \frac{\exp\{-a(p_T + \Delta E)\}}{\exp\{-ap_T\}} = \int d(\Delta E) P(\Delta E) \exp\{-a\Delta E\}. \quad (21)$$

For the spectra of produced quarks and gluons computed from Eq. (15) at RHIC energies, one finds that the logarithmic slope n of the partonic p_T -spectrum increases with increasing p_T . This makes parton energy loss more effective in reducing R_{AA} at high p_T . Moreover, due to kinematic boundary effects, the underlying partonic spectrum at RHIC can be parametrized by an exponential $\exp\{-ap_T\}$ for $p_T \gtrsim 30$ GeV. As a consequence of (21), one thus finds - in agreement with Fig. 3 - an almost p_T -independent R_{AA} at large $p_T \gtrsim 30$ GeV. [Although this is not within experimental reach, we note that close to the kinematical limit $p_T \sim 100$ GeV, the slope decreases even faster.] The remaining weak p_T -dependence can be attributed to the parton species dependence of the quenching weights and to the nuclear dependences of the incoming parton distribution function which turn out to further reduce R_{AA} with increasing p_T . In conclusion, the onset of a perturbative p_T powerlaw (at $p_T > 5$ GeV say), and its return to an exponential spectrum at $p_T \gtrsim 30$ GeV leave a finite window at RHIC energies. Within this window, the gradually increasing slope of the partonic spectrum implies an almost p_T -independent nuclear modification factor.

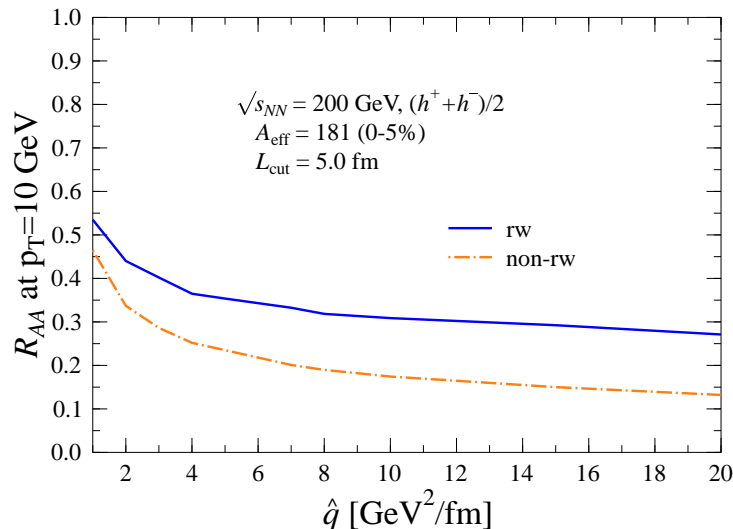


Figure 4: (Colour online) R_{AA} for charged hadrons $h \equiv (h^+ + h^-)/2$ in the 0 – 5% most central Au+Au collisions at $\sqrt{s_{NN}} = 200$ GeV as a function of \hat{q} for $p_T=10$ GeV.

We now turn to the dependence of R_{AA} on \hat{q} . Partons which traverse a larger in-medium pathlength tend to lose more energy. As a consequence, the dominant fraction of leading partons comes from the outer skin of the two-dimensional transverse overlap of the colliding nuclei. We refer to the outer region of the medium as “skin” rather than “surface” since it has a finite three-volume. In Appendix A, we give further support for this dominance of skin-emission for realistic densities at RHIC and at the LHC. The dominance of skin-emission appears to limit the sensitivity of R_{AA} on the density of the medium. Indeed, we find that for sufficiently large but realistic densities of the medium, the thickness of the outer skin changes only weakly with increasing density, see Fig. 4. Thus the nuclear modification factor is a sensitive measure of the density of the medium up to $\hat{q} \lesssim 4 \text{ GeV}^2/\text{fm}$, but it loses this sensitivity for higher values of \hat{q} .

From Fig. 3 and 4 we conclude that the suppression of high- p_T hadrons measured in $\sqrt{s_{NN}} = 200 \text{ GeV}$ Au+Au collisions at RHIC requires a time-averaged transport coefficient $\hat{q} > 5 \text{ GeV}^2/\text{fm}$ and favours $\hat{q} = 5 - 15 \text{ GeV}^2/\text{fm}$.

4 Extrapolation to the LHC

Within the formalism of section 2, the choice of the transport coefficient \hat{q} is the main unknown for extrapolating our results from RHIC to Pb+Pb collisions at the LHC energy $\sqrt{s_{NN}} = 5500 \text{ GeV}$. One expects that this transport coefficient grows linearly with the number density, n_i , of the medium [22, 25], and hence is proportional to the multiplicity per unit rapidity

$$\hat{q} \propto \frac{dN^{\text{ch}}}{dy}. \quad (22)$$

For the LHC, model predictions of the event multiplicity vary by a factor ~ 4 at least [34], but the corresponding uncertainty for R_{AA} may be significantly smaller since R_{AA} changes only weakly for large values of \hat{q} . The second unknown in the calculation of R_{AA} is the maximal lifetime of the dense medium, denoted by L_{cut} . We expect, however, that this choice is numerically unimportant since L_{cut} at LHC is typically larger than the thickness of the effective skin of the medium through which hard partons can penetrate without significant energy loss.

To be specific, we use for the LHC $L_{\text{cut}} = \tau_{\text{QGP}} \sim 10 \text{ fm}$ consistent with hydrodynamical modeling of the time evolution of the medium [35]. We find from an optical Glauber calculation that the 0 – 5% most central Pb+Pb events correspond to the head-on collision of nuclei with $A_{\text{eff}} = 193$. The density estimate is obtained from the EKRT parametrization [36] for which $n_i \sim A^{0.383}(\sqrt{s})^{0.574}$, consistent with the growth of the event multiplicity measured so far. With this input, the transport coefficients at RHIC and the LHC are related like $\hat{q}_{\text{LHC}} = 6.8\hat{q}_{\text{RHIC}}$. For a typical RHIC value, $\hat{q}_{\text{RHIC}} = 10 \text{ GeV}^2/\text{fm}$, we find that $\hat{q}_{\text{LHC}} = 68 \text{ GeV}^2/\text{fm}$ which is one of the parameters used in Fig. 5. In models which predict a smaller multiplicity increase from RHIC to

LHC [34], the suppression is expected to lie in between the bands shown in Fig. 5 for $\hat{q}_{\text{RHIC}} = 10 \text{ GeV}^2/\text{fm}$ and $\hat{q}_{\text{LHC}} = 68 \text{ GeV}^2/\text{fm}$.

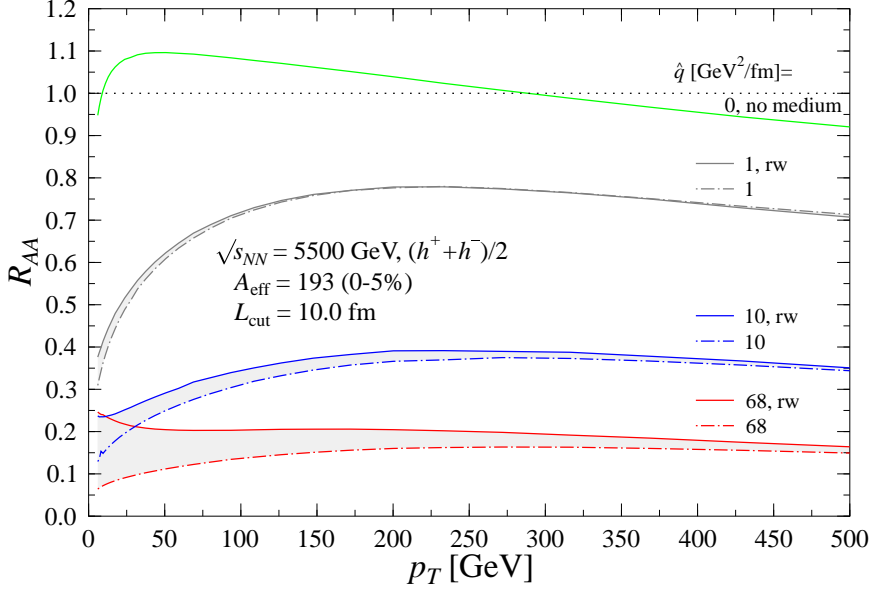


Figure 5: (Colour online) The nuclear modification factor for charged hadrons $h \equiv (h^+ + h^-)/2$ in 0 – 5% most central Pb+Pb collisions at the LHC, calculated for $L_{\text{cut}}=10 \text{ fm}$ and various values of the transport coefficient. The largest value $\hat{q}_{\text{LHC}} = 68 \text{ GeV}^2/\text{fm}$ lies in the range favoured by current multiplicity estimates. See the text for more details.

Based on estimates of the luminosity in Pb+Pb collisions at the LHC and the hadronic cross section, one expects that the nuclear modification factor will be measured up to $p_T \sim 100 - 150 \text{ GeV}$. Not only in this p_T -range but even above, the nuclear modification factor turns out to be almost p_T -independent for $\hat{q}_{\text{LHC}} = 68 \text{ GeV}^2/\text{fm}$. Moreover, it is numerically comparable to R_{AA} at RHIC, calculated for a much smaller transport coefficient. This can be understood as follows: the contribution from the discrete part of the quenching weight to R_{AA} decreases with the increasing transport coefficient from RHIC to the LHC (see Fig. 2 and Appendix A). At the same time, however, since the partonic transverse momentum spectra are steeper at RHIC than at the LHC, the suppression of R_{AA} induced by the continuous part of the quenching weight (parton energy loss) is still larger at RHIC than at the LHC (see discussion in Appendix A). If the density of the medium created at the LHC is significantly reduced ($\hat{q}_{\text{LHC}} = 10 \text{ GeV}^2/\text{fm}$), then one finds a weak but experimentally accessible increase of $R_{AA}(p_T)$ with p_T . The reason is that for sufficiently low density, the probability that partons from deeper layers inside the medium escape with small energy loss grows

significantly with increasing p_T . This effect is even more pronounced for very small densities of order $\hat{q}_{\text{LHC}} = 1 \text{ GeV}^2/\text{fm}$.

From this exercise, we expect that up to the highest transverse momenta accessible at the LHC, leading hadron spectra will show a strong suppression in nuclear collisions. This suppression is likely to result in an almost p_T -independent nuclear modification factor. For the reasons given above and since particle emission from the outer skin of the medium remains essentially unsuppressed even for extreme densities, we expect that the numerical value for R_{AA} at the LHC is comparable to the one at RHIC.

5 The nuclear modification factor at $\sqrt{s_{\text{NN}}} = 62.4 \text{ GeV}$

Experiments at the Relativistic Heavy Ion Collider RHIC have just completed data taking for Au+Au collisions at an intermediate center of mass energy of $\sqrt{s_{\text{NN}}} = 62.4 \text{ GeV}$. In Fig. 6, we give results for the corresponding nuclear modification factor in the present formalism. The main model input is again the value of the time-averaged transport coefficient \hat{q} defined in (5). Based on the multiplicity scaling of the transport coefficient in (22) and the value $\hat{q} \sim 5 - 10 \text{ GeV}^2/\text{fm}$ favoured for RHIC data at $\sqrt{s_{\text{NN}}} = 200 \text{ GeV}$, we chose $\hat{q} \sim 3 - 5 \text{ GeV}^2/\text{fm}$ at $\sqrt{s_{\text{NN}}} = 62.4 \text{ GeV}$. For the second model-dependent input, the life-time L_{cut} of the medium, we chose a slightly reduced value $L_{\text{cut}} = 4 \text{ fm}$. However the dependence of our results on L_{cut} turns out to be negligible for sufficiently large L_{cut} . For medium densities favoured by multiplicity scaling the suppression is pronounced. The results shown in Fig. 6 are, within theoretical uncertainties, consistent with the results published in several recent studies [37, 38, 39].

Some caveats should be kept in mind. First, at intermediate $p_T < 5 - 7 \text{ GeV}$, other physical mechanisms can provide sizeable contributions to R_{AA} . In particular, the anomalous baryon enhancement at intermediate p_T [40, 41] and the Cronin effect [42] are observed to increase R_{AA} . Both contributions may be more pronounced on a spectrum with steeper slope, i.e. for smaller $\sqrt{s_{\text{NN}}}$. Second, the smaller the hadronic p_T , the larger the theoretical uncertainty in calculating parton energy loss. Moreover, below $p_T \sim 4 \text{ GeV}$, the hadron spectra at $\sqrt{s_{\text{NN}}} = 62.4 \text{ GeV}$ deviate significantly from the shape calculated by the collinear factorized pQCD formalism [19].

While completing this work, the first experimental data on the nuclear modification factor in Au+Au collisions at $\sqrt{s_{\text{NN}}} = 62.4 \text{ GeV}$ appeared [43]. These data are for $0.2 < \eta < 1.4$ and $p_T \leq 4 \text{ GeV}$ with $R_{AA}(p_T \sim 4 \text{ GeV}) \sim 0.8 \pm 0.1$ for the 0 – 6% most central bin. Other preliminary data [44] indicate a significant further drop of R_{AA} for $4 < p_T < 6.5 \text{ GeV}$. For the highest p_T , these data are close to the calculation shown in Fig. 6.

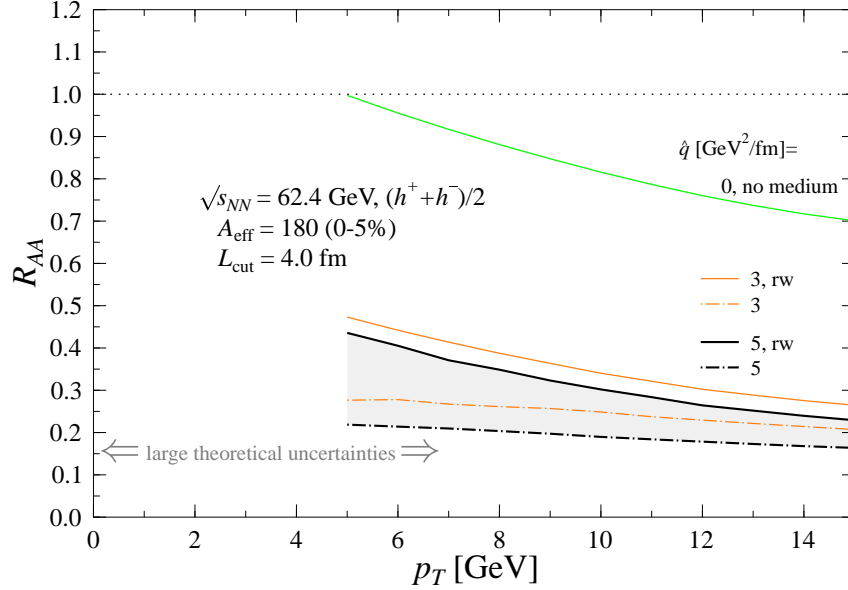


Figure 6: (Colour online) The nuclear modification factor for charged hadrons $h \equiv (h^+ + h^-)/2$ in 0 – 5% most central Au+Au collisions at $\sqrt{s} = 62.4$ GeV. See the text for details.

6 Relating the Transport Coefficient to Energy Density

In section 3, we have shown that RHIC data favour a time-averaged transport coefficient $\hat{q} \simeq 10$ GeV²/fm. This parameter as well as the time-dependent transport coefficient entering eq. (5) scales with the energy density of the medium like [22]

$$\hat{q}_\tau(\tau) = c \epsilon^{3/4}(\tau). \quad (23)$$

Here, c is a proportionality constant which can be calculated for specific models of the medium. In particular, for the model of an ideal quark gluon plasma whose constituents interact perturbatively with the hard parton, we extract this proportionality constant from Figure 3 of Ref. [22]

$$c_{\text{QGP}}^{\text{ideal}} \approx 2. \quad (24)$$

Alternatively, one can determine the constant c from experiment if one has independent information about transport coefficient and energy density. From the measured time-averaged transport coefficient \hat{q} , we find via the dynamical scaling law (5) the transport coefficient for an initial time τ_0 ,

$$\hat{q}_\tau(\tau_0) = \hat{q} \frac{2 - \alpha}{2} \left(\frac{L}{\tau_0} \right)^\alpha. \quad (25)$$

This expression is for an expanding medium with $\hat{q}_\tau(\tau) = \hat{q}_\tau(\tau_0) (\tau_0/L)^\alpha$. We have assumed $\tau_0 \ll L$. The expansion parameter α is unity for a one-dimensional Bjorken expansion and is expected to stay close to unity for realistic expansion scenarios. From this we find

$$c = \frac{\hat{q}_\tau(\tau_0)}{\epsilon(\tau_0)^{3/4}} = \frac{\hat{q}}{\epsilon(\tau_0)^{3/4}} \frac{2-\alpha}{2} \left(\frac{L}{\tau_0}\right)^\alpha \quad (26)$$

For a typical initial time $\tau_0 \sim 0.2$ fm/c, the average in-medium pathlength can be expected to be $\sim 10 \tau_0 = 2$ fm (see Appendix A). The energy density averaged over a uniform transverse profile at initial time τ_0 can be as large as $\epsilon(\tau_0) \sim \mathcal{O}(100 \frac{\text{GeV}}{\text{fm}^3})$, as suggested by the pQCD+saturation+hydrodynamics model [36] which correctly predicted the final multiplicities and transverse energies in central collisions at RHIC [30]. This implies that realistic scenarios lie in the parameter range $\epsilon(\tau_0) < 100 \frac{\text{GeV}}{\text{fm}^3}$, $L \sim 10 \tau_0$, $0.75 < \alpha < 1.5$, for which we find

$$c > 8 \dots 19. \quad (27)$$

Thus, for the entire realistic parameter range, we find a proportionality constant which is a factor $\sim 4 - 5$ larger than the perturbative estimate. We note that \hat{q} is the product of the density of scattering centers times their elastic scattering cross section [22]. Thus, the factor $\sim 4 - 5$ discrepancy observed here is reminiscent of the opacity problem in elliptic flow, where also scattering cross sections much larger than the perturbative ones are favoured by the data [45].

7 Conclusions

In this paper we have studied within the LO pQCD formalism [19] the effect of medium-induced parton energy loss on charged hadron spectra. At high p_T we find generically an almost p_T -independent nuclear modification factor at both LHC and RHIC energies. This is a direct consequence of the interplay of medium-induced energy loss and of a partonic p_T -spectrum whose slope *increases* with increasing p_T . In this approach, an almost p_T -independent R_{AA} is obtained without fine-tuning of nuclear effects (such as Cronin or anomalous baryon enhancement).

For central Au+Au collisions at $\sqrt{s_{NN}} = 200$ GeV, we find a satisfactory agreement with experiment for a transport coefficient in the range $\hat{q} \sim 5 - 15$ GeV²/fm. For these large values of \hat{q} , the nuclear modification factor is only weakly dependent on the transport coefficient, which makes it difficult to constrain the energy density with R_{AuAu} , see Fig. 4. On the other hand, this weakened sensitivity of R_{AA} makes our prediction for the nuclear suppression at the LHC more stable. Irrespective of the uncertainty in the factor by which the density of the medium increases from RHIC to the LHC, the nuclear modification factor is expected to lie in a narrow band $R_{\text{PbPb}} \sim$

0.2 ± 0.1 . This and the almost p_T -independent slope of R_{PbPb} are the main predictions of the present work for Pb+Pb collisions at the LHC. Thus, our calculations indicate that even in a kinematic regime $p_T \sim 100$ GeV where the same energy loss formalism results in jet cross sections which are almost unaffected by the medium [28], the suppression of leading hadron spectra is still sizeable. This points to the importance of resolving the internal structure of jets, i.e. the jet shape and jet multiplicity distributions, at the LHC in order to access the medium-dependence.

In section 6, we have inverted the standard logic of the analysis of nuclear modification factors. Rather than to determine the energy density ϵ from the measured transport coefficient, we extract the proportionality factor $c = \hat{q} \epsilon^{-3/4}$ for realistic upper limit estimates of the energy density. This proportionality factor characterizes the strength of the interaction between the hard (test) parton and the medium. It turns out to be at least a factor $\approx 4 - 5$ larger than expected from perturbative estimates [see discussion of eq. (24)]. Although this perturbative estimate (24) is itself subject to significant uncertainties, we do not expect that this is the only source of such a large discrepancy. Here, we note that our finding is reminiscent of parton cascade studies of elliptic flow [45] where perturbative partonic cross sections have to be scaled by large factors in order to match the size of the collective evolution. Both effects may have a common origin since both concern the interaction strength of partonic degrees of freedom with the medium produced in the collision.

Note added: While completing this work, a calculation of nuclear modification factors in a closely related model appeared [46]. This study supports the approximate p_T -independence of the nuclear modification factor at RHIC and at the LHC. Moreover, this model calculation reproduces the observed centrality dependence of R_{AA} and of the suppression of the away-side jet-like correlations. That the centrality dependence of suppressed high- p_T hadroproduction follows naturally, once the suppression for the most central bin is fixed, was also found in Ref. [47].

Acknowledgements

We thank N. Armesto, R. Baier, A. Dainese and P.V. Ruuskanen for helpful discussions. Financial support from the Academy of Finland, the projects 50338 and 206024, is gratefully acknowledged.

A Further studies of the dependences of R_{AA}

We have argued in section 3 that for the densities attained at RHIC, leading hadroproduction is limited to the outer skin of the collision region. Here, we further support this argument by calculating the dependence of R_{AA} on L_{cut} . In particular, Fig. 7 establishes that a reduction of the maximum in-medium pathlength from 6 fm to 4 fm

leaves the nuclear modification factor almost unaffected. The slight sensitivity of R_{AA} to $L_{\text{cut}}=3$ fm indicates that a small contribution comes from partons which traverse 3 – 4 fm of matter with transport coefficient $\hat{q} = 10$ GeV²/fm. Thus, essentially all partons with $L > 3$ fm, as well as a fraction of the partons with $L < 3$ fm do not contribute to the leading hadron spectrum. The average geometrical path length is larger than $L = 3$ fm, it is $\langle L_{\text{geom}} \rangle = \frac{8}{3\pi} R_A = 5.2$ fm for a cylindrical uniform nucleus (we use $A_{\text{eff}} = 181$ and $R_{A_{\text{eff}}} = 6.2$). Thus, much less than half of the partons will succeed in escaping the medium with sufficient energy, in agreement with the observed value for R_{AuAu} at RHIC.

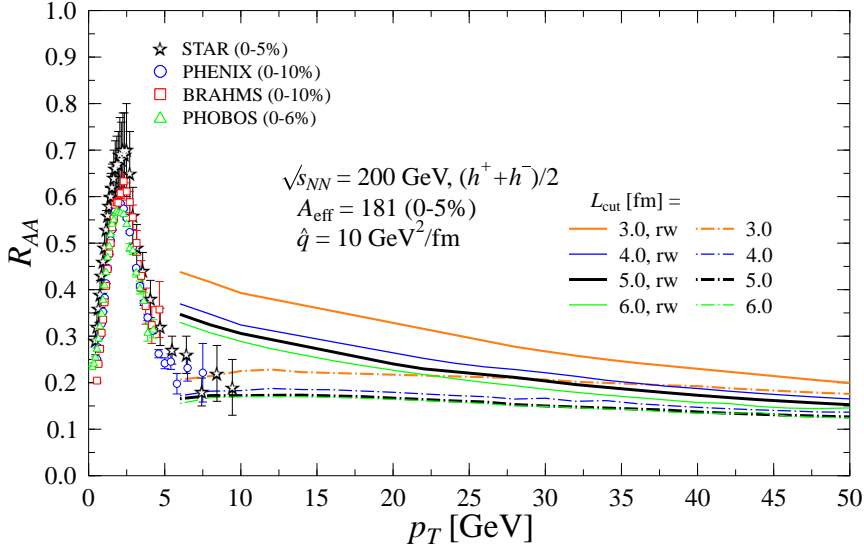


Figure 7: (Colour online) The nuclear modification factor R_{AA} for charged hadrons $h \equiv (h^+ + h^-)/2$ in the 0 – 5% most central Au+Au collisions at $\sqrt{s_{NN}} = 200$ GeV. The solid curves (dotted-dashed curves) are the reweighted (non-reweighted) results with $\hat{q} = 10$ GeV²/fm and $L_{\text{cut}}=3, 4, 5$ and 6 fm. The data are the same as in Fig. 3.

Another illustration of skin-dominated leading hadroproduction in nucleus-nucleus collision is to compare R_{AA} calculated for several *fixed* in-medium pathlengths $L = 1 \dots 6$ fm, see Fig. 8. For a small transport coefficient, $\hat{q} = 1$ GeV²/fm, R_{AA} decreases significantly even for $L=4, 5, 6$ fm, indicating that leading hadrons can originate from partons with significant in-medium pathlength. Fig. 8 is consistent with the statement in [21] that the suppression of hadrons at RHIC can be accounted for by $\hat{q} = 1$ GeV²/fm and $L \sim 6$ fm. In the present study, we find a significantly larger transport coefficient since the relevant in-medium pathlength turns out to be much smaller. Consistent with

the statement made above, if the transport coefficient is increased to $\hat{q} = 10 \text{ GeV}^2/\text{fm}$, partons with in-medium pathlength more than 3 fm make a negligible contribution to the nuclear modification factor, see Fig. 8. This is consistent with the model discussed in Ref. [48]. Effectively, with $\hat{q} = 10 \text{ GeV}^2/\text{fm}$ the results from RHIC can be reproduced with a fixed path length $L \sim 2 \text{ fm}$, which is clearly smaller than $\langle L_{\text{geom}} \rangle = 5.2 \text{ fm}$ (see also [29]). For $L \sim 2 \text{ fm}$, the average momentum transfer acquired by the hard partons is of the order $\sqrt{\hat{q}L} \sim 4.5 \text{ GeV}$. Thus, the direction of partons with $q_{T_i} \lesssim 5 \text{ GeV}$ is randomized; they become part of the medium. This suggests that hadrons with $p_T \lesssim 2 - 3 \text{ GeV}$, which form the bulk of the multiplicity, originate from decoupling of the strongly interacting system. This observation is consistent with the results in [49].

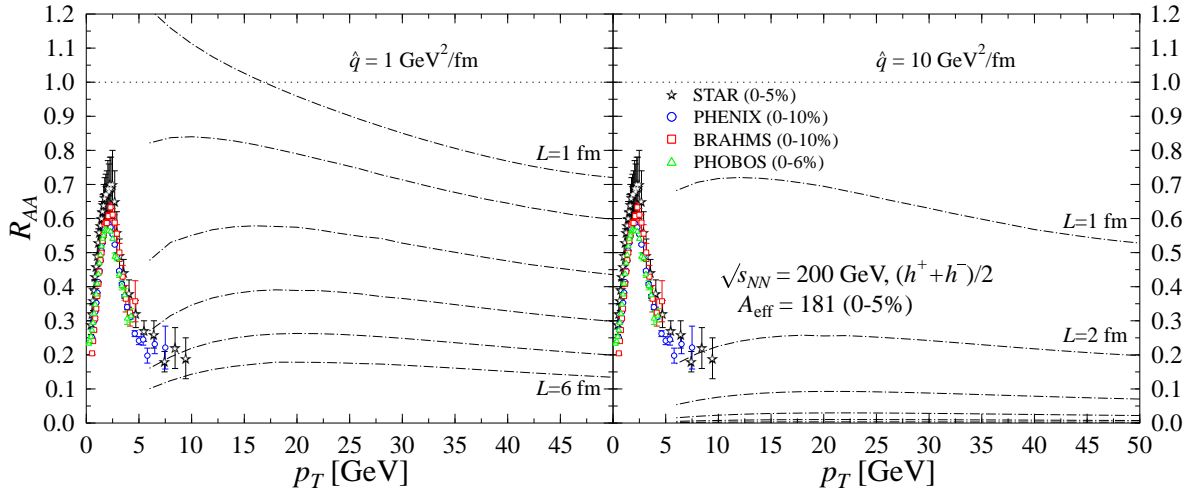


Figure 8: (Colour online) The non-reweighted R_{AA} results at RHIC computed using constant in-medium path length L for $\hat{q} = 1 \text{ GeV}^2/\text{fm}$ (left panel) and $\hat{q} = 10 \text{ GeV}^2/\text{fm}$ (right panel). See the text for further details. The data are the same as in Fig. 3.

We finally check to what extent the effects of parton energy loss on R_{AA} are due to the discrete or the continuous part of the quenching weight (6). The discrete part p_0 depends for fixed L and \hat{q} only on the parton species, see Fig. 2. The non-reweighted contribution of p_0 to R_{AA} therefore interpolates between the values p_0^{gluon} and p_0^{quark} as a function of p_T . In Fig. 9 we fix $L = 3 \text{ fm}$, and show separately the discrete and continuous contribution to the nuclear modification factor R_{AA} at RHIC for $\hat{q} = 1$ and $10 \text{ GeV}^2/\text{fm}$. No other nuclear effects are included in Fig. 9. The high- p_T hadron spectrum at RHIC is dominated by quark production, and thus the non-reweighted discrete component of R_{AA} is very close to p_0^{quark} .

At the LHC, for $\hat{q} = 1$ and $10 \text{ GeV}^2/\text{fm}$, the suppression is weaker than at RHIC, see Fig. 10 and Sec. 4. The contribution of the discrete part to R_{AA} is smaller than at RHIC since a significant part of the hadron production is now of gluonic origin. [The slight decrease of the discrete contribution at $p_T \gtrsim 200 \text{ GeV}$ reflects the relative shape

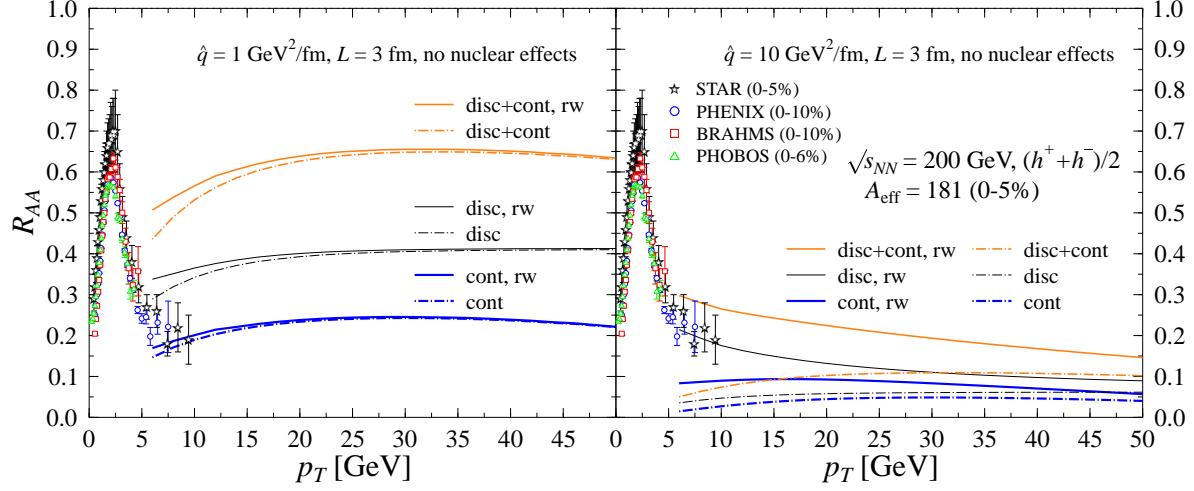


Figure 9: (Colour online) The relative contributions of the discrete and continuous parts of the quenching weight (6) to the nuclear modification factor R_{AA} at RHIC for fixed in-medium path length $L = 3$ fm and for $\hat{q} = 1$ GeV²/fm (left panel) and $\hat{q} = 10$ GeV²/fm (right panel), respectively. The data are the same as in Fig. 3.

of the KKP quark and gluon fragmentation functions at very high z .] The dominant contribution to R_{AA} comes from the continuous part of the quenching weight. Similar to RHIC, the increasing slope of the partonic spectra at high p_T tames the growth of R_{AA} .

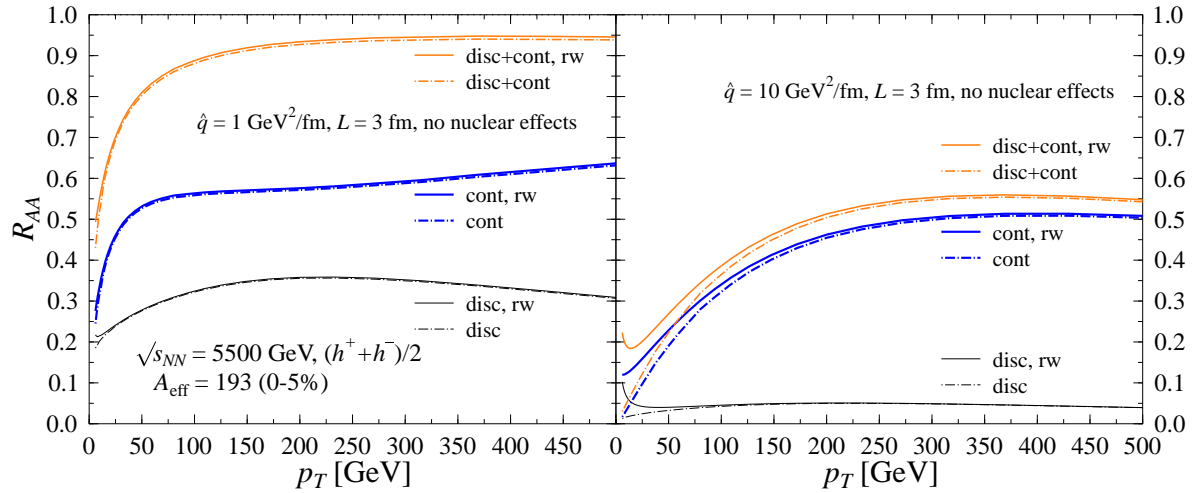


Figure 10: Same as in Fig. 9 for the LHC.

References

- [1] K. Adcox *et al.* [PHENIX Collaboration], Phys. Rev. Lett. **88** (2002) 022301 [arXiv:nucl-ex/0109003].
- [2] S. S. Adler *et al.* [PHENIX Collaboration], Phys. Rev. C **69** (2004) 034910 [arXiv:nucl-ex/0308006].
- [3] C. Adler *et al.* [STAR Collaboration], Phys. Rev. Lett. **89** (2002) 202301 [arXiv:nucl-ex/0206011].
- [4] J. Adams *et al.* [STAR Collaboration], Phys. Rev. Lett. **91** (2003) 172302 [arXiv:nucl-ex/0305015].
- [5] B. B. Back *et al.* [PHOBOS Collaboration], Phys. Lett. B **578** (2004) 297 [arXiv:nucl-ex/0302015].
- [6] I. Arsene *et al.* [BRAHMS Collaboration], Phys. Rev. Lett. **91** (2003) 072305 [arXiv:nucl-ex/0307003].
- [7] C. Adler *et al.* [STAR Collaboration], Phys. Rev. Lett. **90** (2003) 082302 [arXiv:nucl-ex/0210033].
- [8] S. S. Adler *et al.* [PHENIX Collaboration], Phys. Rev. Lett. **91** (2003) 072303 [arXiv:nucl-ex/0306021].
- [9] J. Adams *et al.* [STAR Collaboration], Phys. Rev. Lett. **91** (2003) 072304 [arXiv:nucl-ex/0306024].
- [10] U. A. Wiedemann, arXiv:hep-ph/0402251.
- [11] M. Gyulassy and X. N. Wang, Nucl. Phys. B **420** (1994) 583 [arXiv:nucl-th/9306003].
- [12] R. Baier, Y. L. Dokshitzer, A. H. Mueller, S. Peigne and D. Schiff, Nucl. Phys. B **484** (1997) 265 [arXiv:hep-ph/9608322].
- [13] B. G. Zakharov, JETP Lett. **65** (1997) 615 [arXiv:hep-ph/9704255].
- [14] U. A. Wiedemann, Nucl. Phys. B **588** (2000) 303 [arXiv:hep-ph/0005129].
- [15] M. Gyulassy, P. Levai and I. Vitev, Nucl. Phys. B **594** (2001) 371 [arXiv:nucl-th/0006010].
- [16] X. N. Wang and X. f. Guo, Nucl. Phys. A **696** (2001) 788 [arXiv:hep-ph/0102230].
- [17] X. N. Wang, Phys. Lett. B **579**, 299 (2004) [arXiv:nucl-th/0307036].

- [18] M. Gyulassy, arXiv:nucl-th/0403032.
- [19] K. J. Eskola and H. Honkanen, Nucl. Phys. A **713** (2003) 167 [arXiv:hep-ph/0205048].
- [20] K. J. Eskola, V. J. Kolhinen and C. A. Salgado, Eur. Phys. J. C **9** (1999) 61 [arXiv:hep-ph/9807297].
- [21] C. A. Salgado and U. A. Wiedemann, Phys. Rev. D **68** (2003) 014008 [arXiv:hep-ph/0302184].
- [22] R. Baier, Nucl. Phys. A **715** (2003) 209 [arXiv:hep-ph/0209038].
- [23] R. Baier, Y. L. Dokshitzer, A. H. Mueller and D. Schiff, JHEP **0109** (2001) 033 [arXiv:hep-ph/0106347].
- [24] C. A. Salgado and U. A. Wiedemann, Phys. Rev. Lett. **89** (2002) 092303 [arXiv:hep-ph/0204221].
- [25] R. Baier, Y. L. Dokshitzer, A. H. Mueller and D. Schiff, Phys. Rev. C **58** (1998) 1706 [arXiv:hep-ph/9803473].
- [26] U. A. Wiedemann, Nucl. Phys. A **690** (2001) 731 [arXiv:hep-ph/0008241].
- [27] M. Gyulassy, P. Levai and I. Vitev, Phys. Lett. B **538** (2002) 282 [arXiv:nucl-th/0112071].
- [28] C. A. Salgado and U. A. Wiedemann, arXiv:hep-ph/0310079.
- [29] A. Dainese [ALICE Collaboration], Eur. Phys. J. C **33** (2004) 495 [arXiv:nucl-ex/0312005]; A. Dainese, arXiv:nucl-ex/0311004.
- [30] K. J. Eskola, P. V. Ruuskanen, S. S. Räsänen and K. Tuominen, Nucl. Phys. A **696** (2001) 715 [arXiv:hep-ph/0104010].
- [31] H. L. Lai *et al.* [CTEQ Collaboration], Eur. Phys. J. C **12** (2000) 375 [arXiv:hep-ph/9903282].
- [32] B. A. Kniehl, G. Kramer and B. Potter, Nucl. Phys. B **582** (2000) 514 [arXiv:hep-ph/0010289].
- [33] X. N. Wang, Z. Huang and I. Sarcevic, Phys. Rev. Lett. **77** (1996) 231 [arXiv:hep-ph/9605213].
- [34] N. Armesto and C. Pajares, Int. J. Mod. Phys. A **15** (2000) 2019 [arXiv:hep-ph/0002163].

- [35] K. J. Eskola, H. Honkanen, H. Niemi, V. P. Ruuskanen, S. S. Räsänen and K. Tuominen, in preparation.
- [36] K. J. Eskola, K. Kajantie, P. V. Ruuskanen and K. Tuominen, Nucl. Phys. B **570** (2000) 379 [arXiv:hep-ph/9909456].
- [37] I. Vitev, arXiv:nucl-th/0404052.
- [38] A. Adil and M. Gyulassy, arXiv:nucl-th/0405036.
- [39] X. N. Wang, arXiv:nucl-th/0405029.
- [40] S. S. Adler *et al.* [PHENIX Collaboration], Phys. Rev. Lett. **91** (2003) 172301.
- [41] J. Adams *et al.* [STAR Collaboration], arXiv:nucl-ex/0306007.
- [42] S. S. Adler *et al.* [PHENIX Coll.], arXiv:nucl-ex/0306021; J. Adams [STAR Coll.], arXiv:nucl-ex/0306024; B. B. Back *et al.* [PHOBOS Coll.], arXiv:nucl-ex/0306025; I. Arsene *et al.* [BRAHMS Coll.], arXiv:nucl-ex/0307003.
- [43] B. B. Back [PHOBOS Collaboration], arXiv:nucl-ex/0405003.
- [44] Talks by Takao Sakaguchi [PHENIX Collaboration] and Marco van Leeuwen [STAR Collaboration], 2004 AGS & RHIC Annual Users' Meeting, May 10-14, 2004, http://www.phenix.bnl.gov/~enterria/agsrhic04_hipt/
- [45] D. Molnar and M. Gyulassy, Nucl. Phys. A **697** (2002) 495 [Erratum-ibid. A **703** (2002) 893] [arXiv:nucl-th/0104073].
- [46] A. Dainese, C. Loizides and G. Paic, arXiv:hep-ph/0406201.
- [47] A. Drees, H. Feng and J. Jia, arXiv:nucl-th/0310044.
- [48] B. Muller, Phys. Rev. C **67** (2003) 061901 [arXiv:nucl-th/0208038].
- [49] K. J. Eskola, H. Niemi, P. V. Ruuskanen and S. S. Räsänen, Nucl. Phys. A **715** (2003) 561 [arXiv:nucl-th/0210005].